Article

Specifying the External Impact on Fluvial Lowland Evolution: The Last Glacial Tisza (Tisa) Catchment in Hungary and Serbia

Jef Vandenberghe [1],* , **Cornelis (Kees) Kasse [1], Dragan Popov [2], Slobodan B. Markovic [2], Dimitri Vandenberghe [3], Sjoerd Bohncke [1],† and Gyula Gabris [4]**

[1] Department of Earth Sciences, Vrije Universiteit, 1081HV Amsterdam, The Netherlands; c.kasse@vu.nl
[2] Department of Geography, Tourism and Hotel Management, Faculty of Science, University of Novi Sad, 21000 Novi Sad, Serbia; dpopov@live.be (D.P.); baca.markovic@gmail.com (S.B.M.)
[3] Laboratory of Mineralogy and Petrology, Department of Geology, Ghent University, B-9000 Gent, Belgium; davdenbe@gmail.com
[4] Department of Physical Geography, Eötvös University of Budapest, H-1117 Budapest, Hungary; ferencgyula@caesar.elte.hu
* Correspondence: jef.vandenberghe@vu.nl
† Deceased.

check for updates

Abstract: External impact on the development of fluvial systems is generally exerted by changes in sea level, climate and tectonic movements. In this study, it is shown that a regional to local differentiation of fluvial response may be caused by semi-direct effects of climate change and tectonic movement; for example, vegetation cover, frozen soil, snow cover and longitudinal gradient. Such semi-direct effects may be responsible for specific fluvial activity resulting in specific drainage patterns, sedimentation series and erosion–accumulation rates. These conclusions are exemplified by the study of the fluvial archives of the Tis(z)a catchment in the Pannonian Basin in Hungary and Serbia from the middle of the last glacial to the Pleistocene–Holocene transition. Previous investigations in that catchment are supplemented here by new geomorphological–sedimentological data and OSL-dating. Specific characteristics of this catchment in comparison with other regions are the preponderance of meandering systems during the last glacial and the presence of very large meanders in given time intervals.

Keywords: Tisza; Tisa; Pannonian Basin; fluvial evolution; terrace development; tectonic impact; local conditions; last glacial; OSL-dating

1. Introduction

The impact of climate on fluvial activity and subsequent drainage patterns has long been recognized [1–3] in addition to other external forcing factors, such as tectonic movements, base-level changes and anthropogenic activity. The traditional correspondence between glacial–interglacial cycles and fluvial evolution has been modified over the last few decades, focusing particularly on the important fluvial morphological changes occurring at climate transitions, originally in temperate to periglacial environments [4–6], and later slightly adapted by the same and other authors [7–9] and confirmed by many field cases (e.g., [10] and references therein). Meanwhile, the timing of considerable changes of fluvial evolution at climatic transitions has also been recognized in other climatic zones, such as the monsoonal environment, for instance in China [11,12] and Australia [13]. It has been

called a model of non-linearity as the fluvial action is influenced by the delayed effect of vegetation development with regard to the climatic change driver.

However, progressive fluvial research has demonstrated that the general validity of the climatically driven, non-linear fluvial model may also need some adaptation in specific climate circumstances, e.g., in glacial [14–16] and arctic environments [17,18], Mediterranean environments [19,20] and tropical conditions [21]. Often, external variables, climate and tectonic movements, may play indirect roles. Such semi-direct climate influences are, for example, the development of specific vegetation cover, the degradation of thick snow cover and glacier ice or the presence of frozen ground. Similarly, climate may have a direct impact on the power supplied by the water flow characteristics that determine fluvial discharge, but also indirectly on the sediment delivery to the drainage system (by way of vegetation). Also, the morpho-structural framework and topography, as indirectly imposed by the tectonic setting, give a characteristic identity to the catchment [15,16,22,23]. In particular, the energy of the fluvial system is determined by the river gradient, which consequently represents a most influential factor in the eroding or accumulating character of a river. In addition, several studies consider the complexity of climate cycles with weakly expressed interstadials or stadials [24,25] or climatic episodes of short duration that hindered rivers crossing thresholds [26–28]. Finally, the ultimate morphological result of river action is determined by its preservation potential as an expression of the river's intrinsic evolution [9,26,29].

The present study concerns the Tisza catchment in the Pannonian (Carpathian) Basin of Hungary and Serbia ("Tisa" in Serbian, Romanian and Ukrainian; "Tisza" in Hungarian) (Figure 1), for which different phases of evolution are identified and dated. Some years ago, the first results were published for the middle Tisza in Hungary [30] and for the lower Tisa in Serbia [31]. We compare and extend that research in an adjacent area to the north in the middle Tisza and further downstream in the lower Tisa. This paper aims to illustrate the effects of a specific climatic and topographical setting on fluvial morphological development, namely that of temperate continental climate conditions, in contrast to previous studies, which generally dealt with more oceanic conditions. In addition, a low-relief and thus low-energy topography is considered. This means, with regard to vegetation cover, that a more steppic environment rather than tundra is involved and, with regard to topography, that a low bedload–suspension load ratio is characteristic of this catchment due to its low gradient.
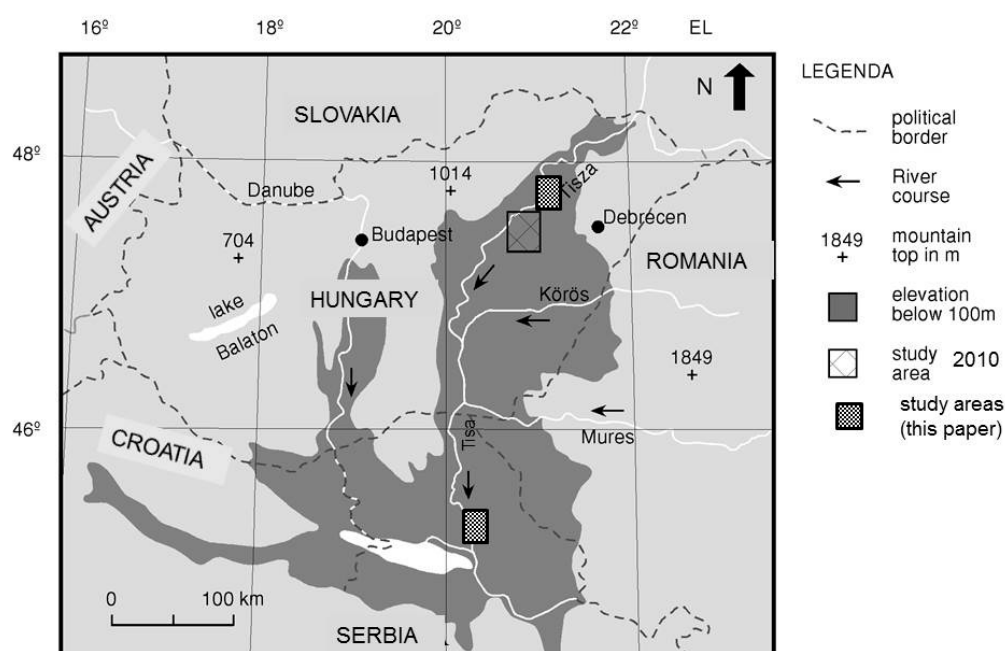

Figure 1. Location map of the Tis(z)a catchment in Hungary and Serbia.

2. Study Region and Previous Research

The Tis(z)a is a major tributary of the Danube, starting its course from the Eastern Carpathian Mountains in Romania, flowing through Ukraine and arriving in the Pannonian Basin in Hungary (middle Tisza) and finally in Serbia (lower Tisa), which is the lowest part of the Basin [32,33]. Both the Danube and Tis(z)a formed their valleys in thick Quaternary basin deposits. Their wide floodplains show an intriguing pattern of successive meandering systems and impressive fluvial deposits from the last glacial and Holocene, extensively described previously [30,34–36].

In comparison with the periglacial-temperate regions further north, the environmental setting in the loess-covered Tisza catchment differed in a few aspects during the late Weichselian. Firstly, the vegetation cover was less dramatically reduced; probably a steppic cover including some persistent tree refugia, in contrast to the bare tundra landscape in the northern coversand regions [37,38]. Secondly, the climate was more continental, with colder winters, warmer summers and less precipitation [39]. Thirdly, the study region coincides with the marginal zone of permafrost at the end of the last glacial, in contrast to NW Europe, which was invariably within the permafrost belt [40,41].

Structurally, the Tisza catchment is situated in the Pannonian basin, a zone of considerable tectonic subsidence [42–44]. On average, the longitudinal gradients in the drainage system of the tectonic basin are very low, from c. 1.86 cm/km in the lower Tisa to 5–10 cm/km in SE Hungary and to 15 cm/km in central–northern Hungary, leading almost entirely to suspension transport currently [30,31,35]. The evolution of the drainage system was obviously determined by the particular tectonic subsidence pattern during the Pleistocene. In addition, this tectonic impact was supplemented by evident climatic overprints [30,35,36,45–47].

3. Methods

Following the original research set-up applied by Kasse et al. [30], information on the sedimentary architecture was acquired by topographic (DEM) analysis and field investigations, mainly consisting of transects across the present floodplain using hand-drill data and a few geoelectric sections. Detailed coring enabled the reconstruction of the precise geometry of former, now abandoned channels. A semi-closed gouge and suction-tube corer were used in the water-saturated sediments. Drill coring was supplemented with exposure data from sand or clay exploitation pits. Apart from palynological analyses [30], sedimentological analysis involved grain-size measurements by laser diffraction. The preparation method of the grain-size analyses involved, for instance, the removal of calcium carbonate and organic material by adding HCl and H_2O_2, respectively [48]. It initiated, amongst others, a clay–silt boundary at 8 μm, which we apply here.

Our previous work in the Tisza basin demonstrated the complexity of interpreting chronologies derived from radiocarbon dating because of the possible and uncertain degree of reworking [30]. The present project therefore explores the possibilities of luminescence dating. Luminescence research in the Hungarian fluvial domain has been summarised previously [36]. The first results in the Serbian domain focused on the methodology (involving infrared stimulated luminescence—IRSL—signals from K-feldspar) that was used for dating a sequence of aeolian and fluvial deposits as exposed in the sandpit at Mužlja [49].

In this study, four additional optically stimulated luminescence (OSL) samples were collected from a sequence of floodplain deposits exposed at a section at Zrenjanin, of which three could be dated using OSL signals from fine-sand sized (63–90 μm) grains of quartz. These samples were prepared in the usual manner (HCl, H_2O_2, sieving, density separation, HF) and mounted on the inner 8 mm of 9.7 mm stainless steel discs using silicon oil as adhesive. Luminescence measurements were made using automated Risø readers (Risø National Laboratory, Roskilde, Denmark) equipped with blue (470 nm) and IR (870 or 875 nm) LEDs; all luminescence signals were detected through a 7.5 mm thick Hoya U-340 filter (details of the luminescence equipment can be found in Bøtter-Jensen et al. [50] and Lapp et al. [51]). The purity of the quartz grains was confirmed by an OSL IR depletion ratio consistent with 1.0 ± 0.1 [52]. Equivalent dose (D_e) determination was carried out using the single-aliquot

regenerative-dose (SAR) protocol [53,54]. Optical stimulation with blue diodes was undertaken for 38 s at 125 °C. The initial 0.31 s of the decay curve, minus a background evaluated from the 0.31–1.08 s interval, was used in the calculations. The measurement of the test-dose signal was preceded by a reduction in heat (cut-heat) to 160 °C and followed by a high-temperature cleanout by stimulation with the blue diodes for 38 s at 280 °C. D_es were calculated from the flat 160–260 °C region in a plot of D_e versus preheat temperature ("preheat plateau"; the duration of the preheat was 10 s). For one of the samples, the dependence of the measured dose on preheat temperature was also investigated through a dose recovery test [54]. Natural aliquots were bleached using the blue LEDs at room temperature (two times 250 s, with a 10 ks pause between), given a dose close to the estimated D_e, and measured using the SAR protocol as outlined above. Three aliquots were measured at each of seven different preheat temperatures in the range of 160–280 °C. For all samples, a dose recovery test was also performed for a preheat of 220 °C only, but using a higher cut-heat to 200 °C. Low-level high-resolution gamma-ray spectrometry was used for the determination of the natural dose rate (see [55,56] for details). For this, the sediment collected around the OSL tubes was dried at 110 °C (until at a constant weight), homogenized and pulverized. A subsample of typically ~140 g was then cast in wax [57] and stored for one month before being measured. The radionuclide activities were converted to dose rates using tabulated conversion factors [58]. Based on Mejdahl [59] and Aitken [60], a factor of 0.9 (±5% relative uncertainty) was adopted to correct the external beta dose rates for the effects of attenuation and etching. An internal dose rate of 0.013 ± 0.003 Gy ka^{-1} was assumed [61]. Dose rates were corrected for the effect of moisture, assuming a time-averaged moisture content of $20 \pm 5\%$. The contribution from cosmic rays was calculated [62]. Uncertainties on the luminescence ages were calculated following the error assessment system proposed by Aitken [63,64], using contributions from quantified systematic sources of uncertainty [56,65].

4. New Results

4.1. Middle Tisza (NE Hungary)

We complete the former description of the middle Tisza system [30] by adding the sedimentology and morphology of a large meander further upstream near Tiszacsege (Figures 2 and 3). That meander, belonging to system 3b (see below), together with a few neighbouring meanders of similar size (e.g., at Ujszentmargita; Figure 3), is eroded into the sediments of the previous meandering system 1 comprising, for instance, the Meggyes meander (Figures 2 and 3). A detailed drilling section along the axis of the Tiszacsege meander bend shows the development and appearance of a typical meander bend. It consists morphologically of a series of ridges and swales and an outer deep abandoned channel (Figure 3). The latter channel marks the final stage of that meander development before it was cut off. The entire area is covered with a veneer of clayey silt, often consisting of alternating laminae of sandy silt and clay, interpreted as flood sediment from the contemporaneous and/or younger river. The top of the ridges may be up to 3 m higher than the swales in between. They consist of vertical sets of weakly laminated, fining-upwards sediment sequences from coarse (gravelly) to fine silty sands (Figure 4), with each individual set reaching a maximum thickness (when not eroded) of 2–3 m. The depressions between them show a similar sediment sequence, except that the upper clayey–silty cover is generally thicker than on top of the ridges, which means that the topography predating the ultimate flooding of the areas was even more pronounced than it is at present. From the morphology, sedimentology and position within the meander bend, these forms and sediments are obviously interpreted as a series of (high) scroll bars (point bars) leaving a depression successively between each of them and its neighbours. The youngest channel of the system is filled, after abandonment, with up to 15 m of similar fine-grained sediment as the upper flood sediment that covers the point bars, but more humic and containing molluscs. The pollen diagram of Tiszacsege is located at the maximum curvature of this abandoned channel; it starts in the final phase of the Pleniglacial [30].
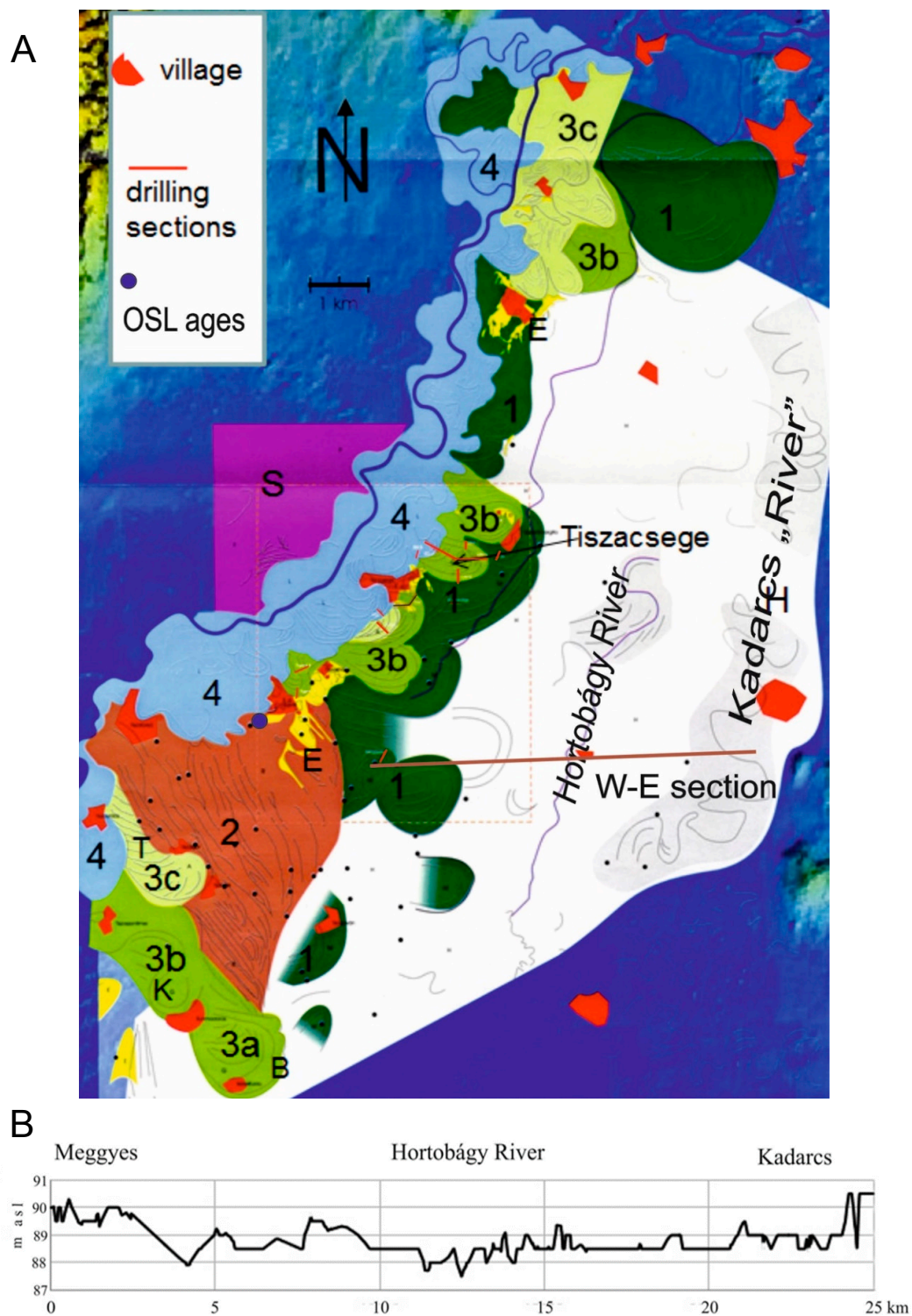
Figure 2. (**A**) Morphological map of the middle Tisza area. H: Hortobagy system; E: aeolian forms (yellow); 1–4: fluvial systems (see text); 3a-b-c: Berekfurdo (B), Kunmadaras (K), Tiszaörs (T) meanders in the lower left corner (from Mol et al. [10]); S: Sajo alluvial fan; W-E section, see B; (**B**) topographic W-E section through the Hortobagy plain (white color in A), including the old Kadarcs system, and the Meggyes meander (system 1 of the younger valley belt).
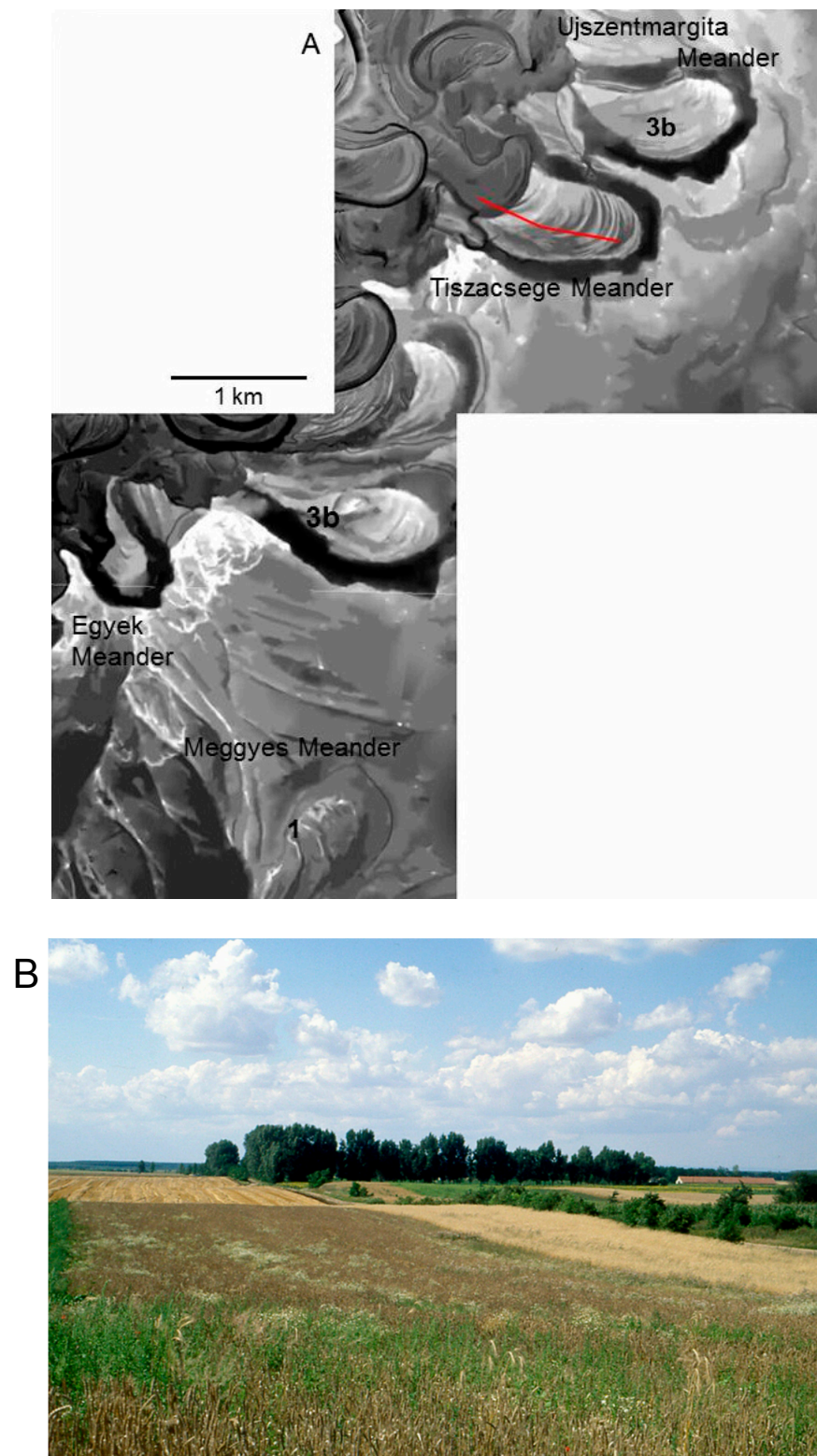
Figure 3. (**A**) Orthophoto of the study area in the middle Tisza (location see Figure 1). (**B**) Photo shows the swale and ridge topography in the meander bend of Tiszacsege.
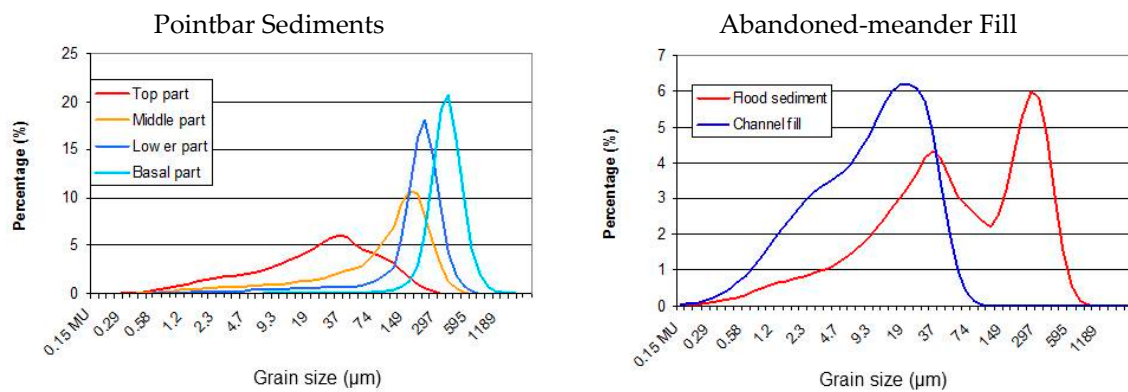
Figure 4. Typical grain-size distributions of point bar, flood and channel fill sediments of the Tiszacsege meander (middle Tisza). The left diagram shows a representative grain-size evolution in one individual point bar (at depths of 6.50, 5.20, 4.60 and 3.80 m). The right diagram shows the grain-size distribution in the centre of the last abandoned channel of max. 15.5 m depth (flood sediment from the upper 2 m, channel fill at c. 8 m depth).

Detailed grain-size information from the point-bar series and the channel fill is represented in Figure 4. An upward decreasing grain size typifies the sands of point bars [66]. The upper flood sediments generally contain a fraction with a mode around 40 μm (the red (top sediment) curve in the left diagram of Figure 4), which is the typical mode for loess deposits in this region [67,68], thus easily interpreted as reworked (alluvial) loess deposits [69]. In addition, the flood sediment often also contains a sand fraction (most obvious in the right panel of Figure 4) indicating some flow on top of the previous floodplain [69,70]. The channel fill shows a clear bimodality (Figure 4, right panel): one fraction is a fine silt of c. 19 μm, corresponding with the fine component in the regional loess cover [67,68] and preferentially settled in the standing water of the abandoned meander, in contrast to the coarser-grained silt (40 μm) which is dominant in the flood sediments; the second fraction is a clay (c. 2 μm) which can only be deposited by settling in standing water ('lacustro-aeolian loess' [69]).

4.2. Lower Tisa (Serbia)

The former morpho-sedimentary research [31] is extended here by additional field and laboratory investigations. Three sections approximately perpendicular to the present Tisa River were investigated mainly by hand drilling supplemented with some exposures [71]. A series of meander systems may be distinguished, sharply dissecting the Titel plateau in the west (at 110–130 m a.s.l.) and the Tamiš plateau in the east (at >82 m a.s.l.), both consisting of Late Pleistocene loess [68,72–74]. The Zrenjanin section is the most representative, crossing three terrace levels (location Figure 5). As in the case of the middle Tisza, the different systems were distinguished by elevation and are separated by distinct erosive meander scarps.

The oldest fluvial series, mainly consisting of large meanders, may be subdivided into systems (1), (3a) and (3b), all situated approximately at the same elevation of c. 79–81 m a.s.l.; a system (3c) slightly lower at 78–79 m a.s.l.; and a youngest one a few metres lower (system 3d at c. 75 m a.s.l.). Clearly separated from these series of large meanders is a series of small meanders (system 4), which are not further subdivided, at 72–75 m a.s.l. elevation (Figure 5).
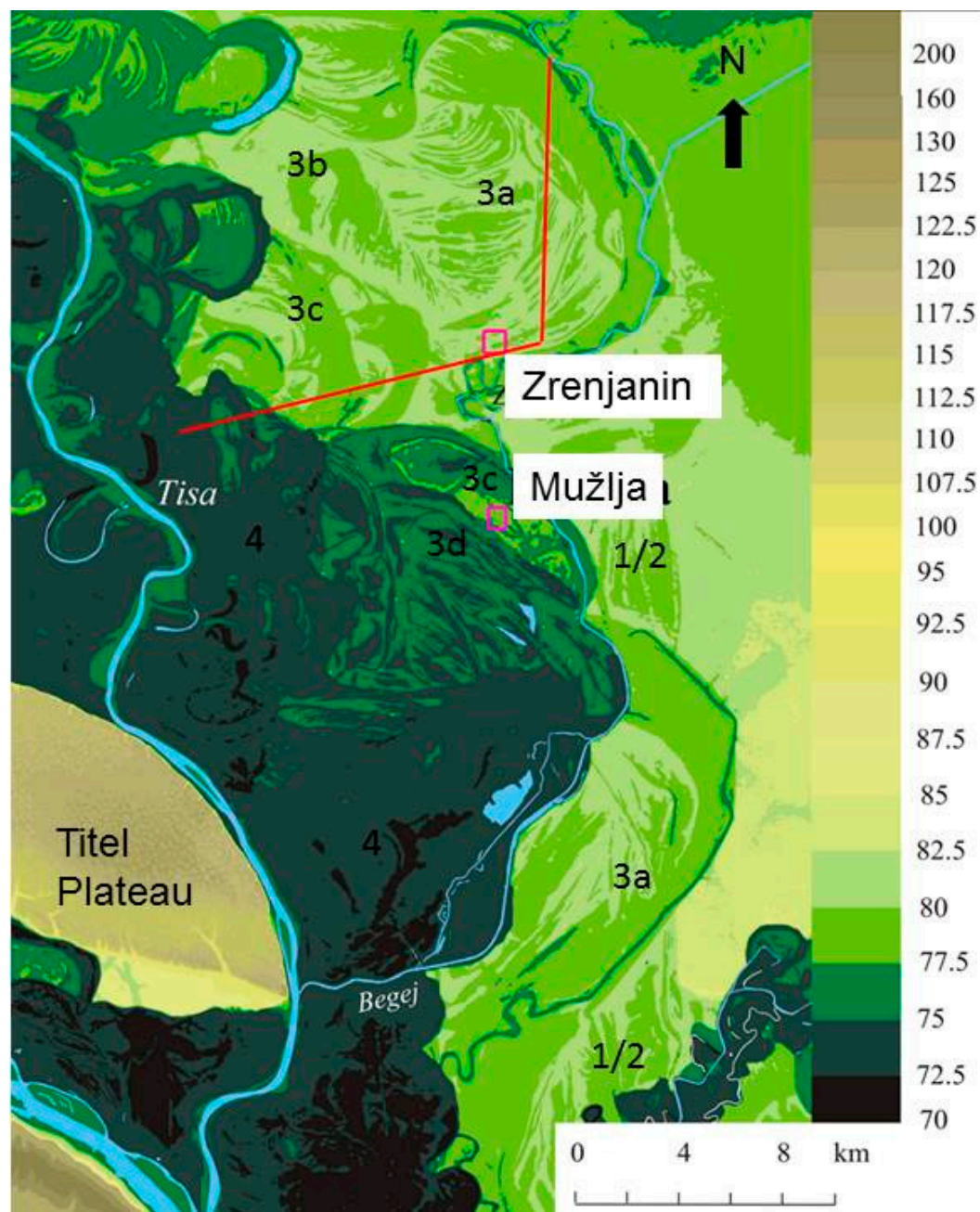
Figure 5. Morphological map of the study area in the lower Tisa comprising the terrace systems 1, 3 and 4 incised in the loess plateaus at both sides of the river. The system (2) braided pattern from Hungary (level B, unit 2) is absent here. The squares indicate the locations of the exposures at Zrenjanin and Mužlja. Height scale in m a.s.l.

In general, each terrace level shows the same morpho-sedimentary expression as in the Tiszacsege meander described above. Morphologically, there is a clear succession of ridges and depressions, interpreted as point bars and inter-bar swales, respectively. Both are covered by a sheet of clayey flood sediments. somewhat thicker than their equivalents in the middle Tisza (1.5 to 3.5 m). The underlying point-bar facies consist of individual sets of 1 to 3 m thick fining-upward sediment ending at their top in gyttja or clay (in the middle Tisza, these very fine capping sediments are missing, except in the abandoned channels) and occasionally containing shell debris and coarse sand grains at the bottom. They are interrupted by channels to a depth of 12 m, often at the outer edge of a terrace level. Following

abandonment, the latter channels have been filled mainly with similar fine-grained sediments as the flood cover, i.e., (clayey) silt or fine sand at the base covered by (humic) silt-clay with sand laminae and ultimately clay–silt without sand. The lowest fill-sediments may occasionally contain poorly sorted sand beds.

An exposure at Zrenjanin (location Figure 5) enabled the detailed study and sampling of the sedimentary structures in the 2–6.5 m thick, fine-grained sediments that occur at the top of the series in meander system 3a (Figure 6). There is a gradual transition to the underlying sediments, which contain more sand and were cored by hand-drilling to a depth of 10.7 m below the surface. The sediment series is described according to sedimentary structures and grain-size composition:

- 0–2.30 m: clay-rich silt (c. 30% clay) with uniform grain-size composition, a modal size of c. 30 μm and almost completely free of sand (Figure 7A). A chernozem soil (1 m thick) is formed at the top while a brown-rusty soil with prismatic structure is present between 1.70 and 2.00 m (Figure 6);
- 2.30–2.80 m: a clay-silt sediment without any sand and a modal size of 10 μm, horizontal, and finely laminated (Figures 7A and 8A). The transition to the overlying sediment is gradual with bimodal laminae, and similarly the transition to the underlying layer is gradual;
- 2.80–5.20 m: alternating thin beds consisting of clay-rich fine-to-medium or coarse silt without sand (350 cm in Figure 7A) and obliquely bedded silty sand layers (up to 20% sand, modal values of 20 and 50 μm) (Figure 8A). The sand beds become thicker towards the base of this unit (ranging from a few centimetres to a few tens of centimetres thick), showing small but clear cross-laminated ripples pointing to a westward water flow (Figure 8B). The lower boundary of these sand beds is mostly sharp (erosive). Calcium carbonate nodules are frequently present, as well as mica grains on the bedding surfaces. A layer between 5.20 and 5.80 m shows a transitional grain size to the underlying layer;
- 5.80–6.50 m: horizontal, finely laminated, silty fine sands with modal values between 55 and 80 μm (Figure 7B) alternating with silt–clay beds (a few tens of centimetres thick) with sharp upper boundaries. Convoluted deformation at the scale of tens of centimetres resulting from liquefaction is seen in the silt–clay beds; a periglacial origin is not obvious. Gradually changing (6.50–7.00 m) to 7.00–8.70 m: sandy beds coarsening to >100 μm modal values with occasional coarse-sand fractions and decreasing silt and clay content, alternating with silt–clay beds (Figure 7B);
- 8.70–10.70 m: two clearly developed fining-up sand series (Figure 7C).

Figure 6. *Cont.*

Figure 6. Top of the section at Zrenjanin in the upper sediments of a large meander. Notice the chernozem soil at the surface and a soil at 1.7–2.00 m depth with prismatic structure. Sampling depth (base of exposed section) is at 6.90 m.
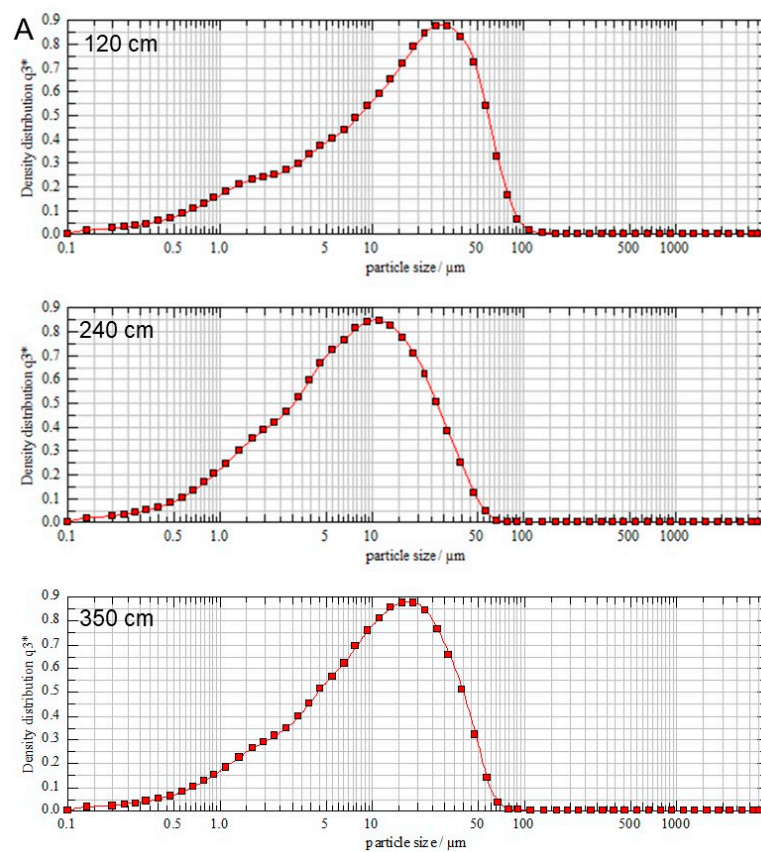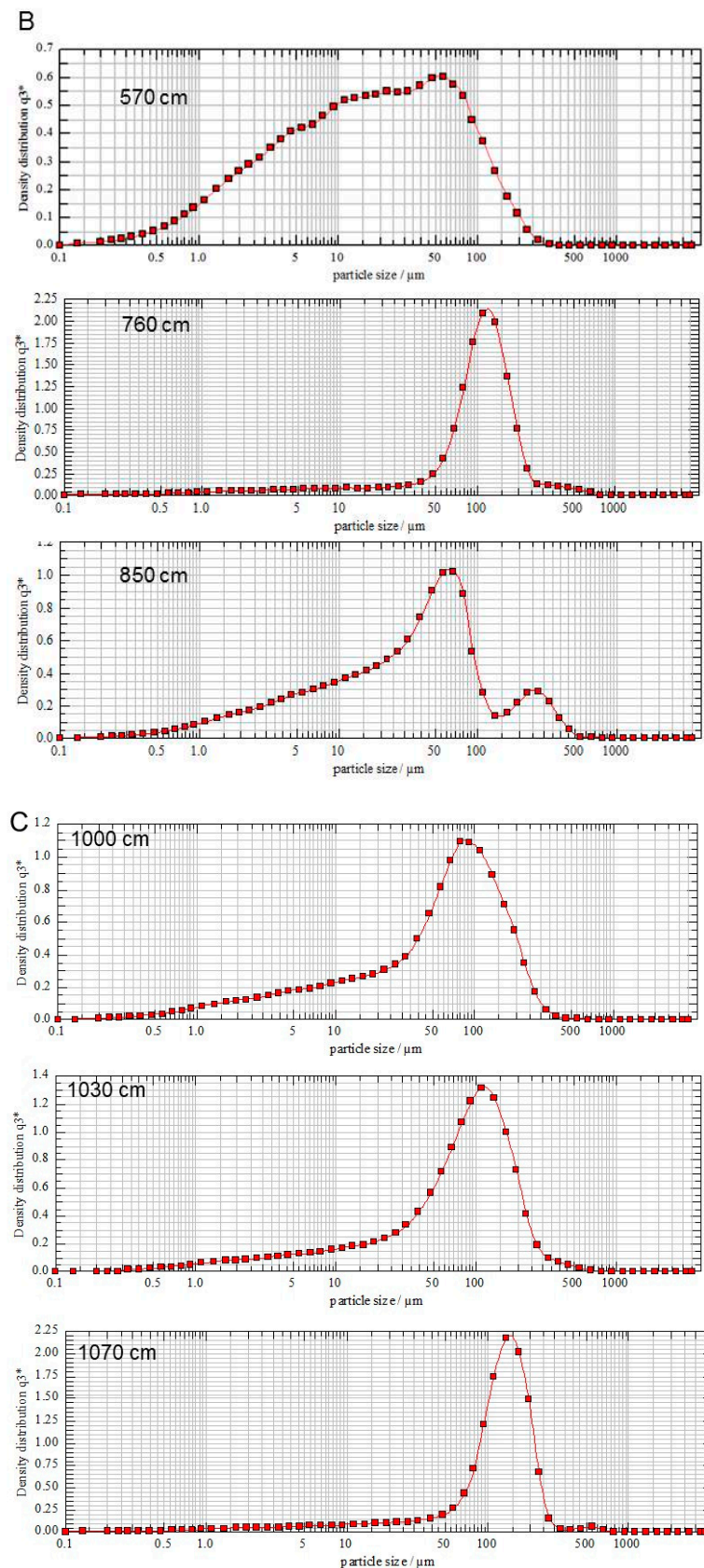

Figure 7. *Cont.*

Figure 7. Grain-size distribution curves of the sediments in the meander system of Zrenjanin (location in Figure 5); depths in cm below surface. (**A**) different facies in the exposed upper silty floodplain sediment; (**B**) grain-size distributions from drilled laminated sandy–silty sediment (channel fill) at the same location; (**C**) grain-size distributions from a drilled fining-upward point-bar series. q3* is a volumetric density parameter equivalent with the distribution frequency.
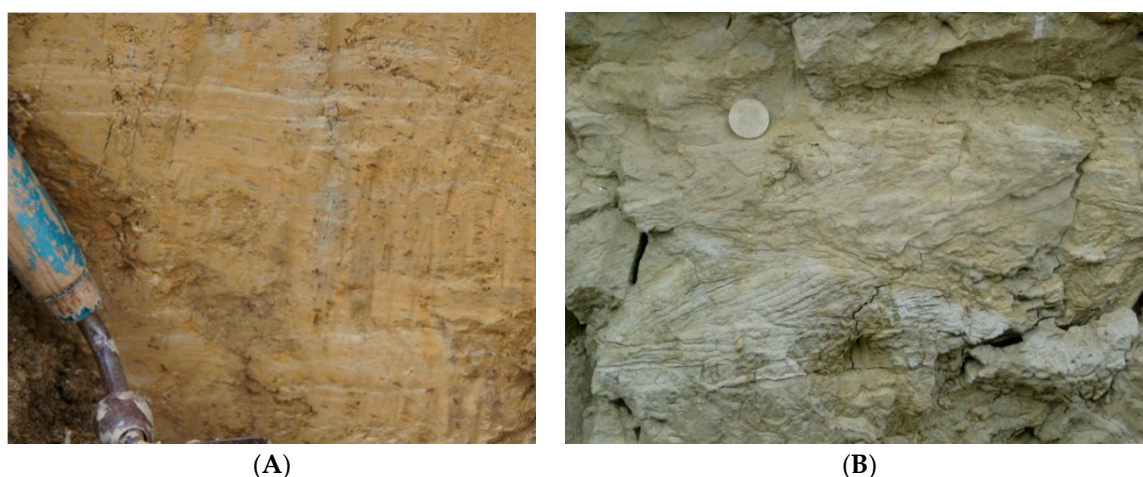
(A)   (B)

Figure 8. Sedimentary structures in the section at Zrenjanin: (**A**) finely laminated clay–silt (2.30–2.80 m); (**B**) cross-laminated ripple bedding in fine silty sand at c. 4 m depth.

The lowest unit (8.70–10.70 m) is interpreted as a typical facies of channel and point-bar deposits within an actively meandering system. The facies of heterogeneous, poorly sorted sands and silts between 7.00 and 8.70 m shows characteristics of upper point-bar deposits. The upper 6.50 m fine-grained sediments are interpreted as channel fills or accumulation in the floodplain of a meandering system that formed in between the point bars of system 3a (see below and Figure 5).

Samples for quartz-based SAR-OSL dating were taken at 5.40 m in homogeneous silt–clay, 6.10 m and 6.60 m in cross-laminated sand, and at 6.90 m in a silt–clay bed. The uppermost sample yielded insufficient fine-sand quartz for OSL-analyses. The results for the other three samples are summarised in Table 1. An internally consistent set of OSL-ages was obtained (33–32 ka), showing no variation with depth. Given the depositional context of the samples and the multiple-grain mode of analysis (see above), the results are to be interpreted as maximum ages. It has been argued, however, that incomplete resetting is rarely a significant source of inaccuracy for the ages under consideration [75]. A dose-response and OSL-decay (inset) curve for an aliquot of sample GLL-150803 are shown in Figure S1. To describe the dose-response curves, we used either a single or the sum of two single saturating exponential functions. D_e values exhibit no systematic dependence on preheat temperatures in the range of 160–260 °C (see Figure S2); across this region, recycling ratios are generally consistent with 1.0 ± 0.1, and values for recuperation remain comfortably below 0.5% of the sensitivity-corrected natural signal. The dose-recovery test yielded an average measured to given dose ratio (± 1 standard error) of 1.13 ± 0.03 across the 160–260 °C preheat temperature range ($N = 18$; sample GLL-150803; Figure S3). This implies that a known laboratory dose, administered following bleaching but prior to heating, cannot be measured to within 10% and is systematically overestimated by about 10%. Increasing the cut-heat temperature to 20 °C below the preheat temperature did not improve our ability to recover a dose; a dose recovery test using a preheat temperature of 220 °C (chosen as the approximate middle of the preheat plateau) and a cut-heat to 200 °C yielded a value of 1.15 ± 0.05 ($n = 9$; three aliquots for each sample). This behaviour, and its relevance as to the accuracy of measurements of natural doses, remains to be understood. Combining these finds with our earlier results [49] indicates that the possibilities of OSL dating using quartz may be limited; future studies may therefore seek to investigate the potential of K-feldspar.

Table 1. Radionuclide concentrations used for dose rate evaluation, estimates of past water content, calculated dose rates, D_es, and calculated ages (Zrenjanin). The dose rate includes the contributions from internal radioactivity and cosmic rays. The uncertainties mentioned with the D_e and dosimetry data are random; the uncertainties on the ages are the overall uncertainties, which include the systematic errors. All uncertainties represent 1s.

Field Code	GLL Code	^{234}Th (Bq kg^{-1})	^{226}Ra (Bq kg^{-1})	^{210}Pb (Bq kg^{-1})	^{232}Th (Bq kg^{-1})	^{40}K (Bq kg^{-1})	Water Content (%)	Dose Rate (Gy ka^{-1})	D_e (Gy)	Age (ka)
ZR 6.10	GLL-150802	33 ± 3	38.5 ± 0.6	35 ± 2	44.0 ± 0.3	605 ± 4	20 ± 5	2.82 ± 0.02	92 ± 5	32 ± 3
ZR 6.60	GLL-150803	29 ± 1	31.5 ± 0.5	34 ± 2	36.6 ± 0.4	445 ± 3	20 ± 5	2.27 ± 0.02	74 ± 3	33 ± 3
ZR 6.90	GLL-150804	31 ± 2	34.7 ± 0.5	33 ± 2	42 ± 0.4	624 ± 4	20 ± 5	2.80 ± 0.03	90 ± 6	32 ± 4

The lateral erosion scar of meandering system 3d enabled the study of an exposure in the sediments of system 3c at Mužlja (location Figure 5). This 4 m deep exposure is located only a few meters from the section that had previously been sampled for luminescence dating [49]. The sediments underlie a point bar of that system. In general, they are finely and horizontally laminated fine-grained sands, occasionally silty and cross-laminated.

Below a 1 m thick Holocene chernozem soil is a fine-grained sand, in general finely and horizontally laminated, with slightly more silty beds at 1.30–1.50 m and 1.70–1.80 m depth. Slightly coarser sand, mica-rich with low-angle cross-lamination and containing some pebbles of mm size, occurs at depths of 2.70–2.80 m and 3.10–3.25 m (Figure 9). The presence of a 2 cm thick, finely laminated, clayey silt bed is striking. The origin of this 4 m sediment series is not readily obvious: their spatial and stratigraphic position would suggest a fluvial point-bar origin, but no current flow structures were found, and a local dune blown up from point-bar deposits is not excluded. However, the nearby section used for the OSL-sampling (Figure 9) shows clearer channelling structures (concave-down discontinuous boundaries, cross-lamination of dm size) and ripple cross-lamination, thus favouring a (low-energy) fluvial interpretation of the deposits in the exposure.
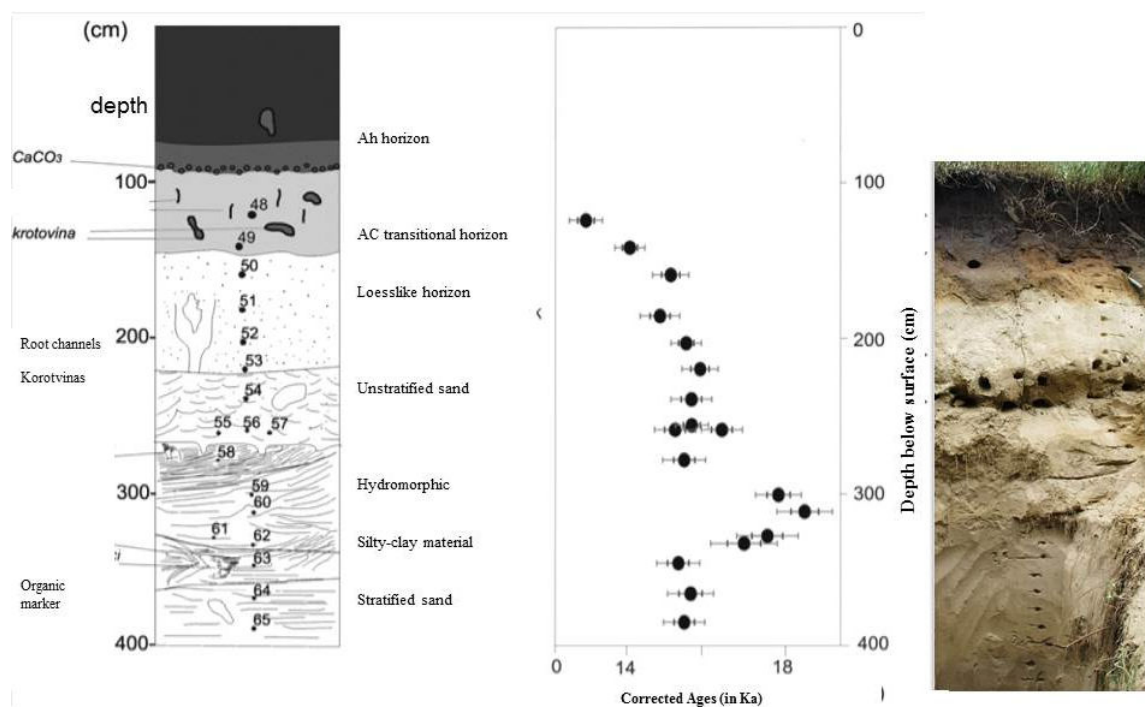

Figure 9. The Mužlja section showing sediments of the meander system 3c (location Figure 5); description of sedimentary structures and lithology, and IRSL dates from Popov et al. [49] with x-axis in ka.

IRSL-dating of K-feldspar provided an age of 15.3–15.6 ka for the deposition of the point bars of that specific meander system [49] (see Figure 9).

5. Identification and Age of the Different Phases of Fluvial Evolution

As a result of the dominant regional subsidence of the Pannonian Basin, the different phases of fluvial evolution are only weakly manifested by height differences, and no real terrace staircase landscape was formed. Some of these phases terminated their accumulation at a similar elevation and can only be distinguished from each other by erosional contacts or the dissection of the older fluvial morphological patterns. An additional difficulty in the sedimentary record is that, in general, all sediments of a specific evolution phase are covered by floodplain deposits of (a) younger phase(s) of fluvial activity as a consequence of the subdued morphology. Finally, as previously discussed extensively [30], both meander-fill and floodplain deposits may give radiocarbon ages that are too old due to the reworking of older organic deposits.

Originally, the Tisza occupied a position near to the eastern margin of the Pannonian basin during the Early–Middle Pleistocene [35]. Due to relatively more intense subsidence in the central part of the basin, the river shifted its position during the late Pleistocene in a westward direction to its current valley [33]. Remnants of the last drainage system before the Tisza reached its present-day valley occur in a subparallel belt east of the present valley (Kadarcs River), occupied in the Holocene by the Hortobagy River, and consist of a series of sinuous channels (grey shaded areas H in Figure 2).

In the Hungarian sector, the surface of the oldest part of the present valley (system 1; meander at Meggyes, Figure 3) is—similar to the precursor of the modern Tisza—morphologically weakly expressed due to the cover of younger vertical floodplain accretion (unit 1 and level A in Kasse et al. [30]). Remnants of sinuous channel scars and point bars with differing orientations suggest formation by a meandering river, as in the Kadarcs system. The humic clay with soil characteristics at the top of this floodplain deposit yielded uncalibrated radiocarbon ages of 24.7 to 22.2 ka BP for autochthonous organic matter (supported by dating of the alkali extract [30]). Since this alluvial clay–soil complex (unfortunately without pollen) probably represents the ultimate phase of floodplain deposition, we infer that the age of activity of this system was prior to that date: i.e., older than c. 28 ka cal BP. The oldest parts of the lower Tisa valley system in the Serbian sector are only represented by two very small areas at c. 80 m altitude (Figure 5: level 1/2). Morphologically, this oldest level of the present-day system shows alternating parallel ridges and swales with an indistinct or slightly curved pattern (Figure 5). No age information is available, preventing correlation with the middle Tisza.

The next and younger phase (2) in the middle Tisza region is represented by a braid plain consisting of straight to slightly curved ridges. The radiocarbon dates from these deposits range from 18,010 BP (bulk detritus) to 13,560 BP (snails) [30], which means a (calibrated) age of c. 22–17 ka (see also discussion below). This system cuts through the large meander system 1. More recently, aeolian sands occurring on top of these fluvial deposits were dated ([36], Figure 8; slightly modified by Novothny) at −27–21.5 ka (OSL/IRSL). System 2 has been previously interpreted as the southernmost extension of the Sajo alluvial fan and may thus be of local, rather than general, importance [33,76].

There then follows a characteristic series of meanders (3) in a belt of the present-day Tisza valley that is approximately at the same altitude as the oldest meanders (system 1; level C at 88–90 m a.s.l. in the middle Tisza [30] and at c. 80 m a.s.l. in Serbia) and the braided system 2. The morphology is characterized by well-developed point bars with ridge-and-swale topography and clear sinuous erosive scars, pointing to lateral migration which has often led to neck-cut-offs. The point bars consist of fine sandy deposits occurring in a series of fining-upward sequences. Abandoned channels are always filled with, occasionally humic, fine sandy to clayey silts, as in Figure 7A. Different generations (3a–d) may be distinguished morphologically in this belt by the successive lateral erosion of previous meander remnants and by progressively decreasing meander wave length. Lateral erosion is accompanied with distinct channel incision, and the deepest meander channels reach considerable depth (up to 15 m).

The correlation of remnants of meander generations is not easy, not least because of the difficulties associated with radiocarbon dating.

Based on the relative magnitude of the meanders and their morphologically relative age, we correlate the oldest and largest meanders of that phase (3a) in the lower and middle Tis(z)a with each other, i.e., the meander of Zrenjanin with the meander of Berekfurdo. The meanders that formed during that first phase have a remarkably large wavelength, although exact determination is difficult (in the Hungarian sector it is estimated at c. 6–10 km at Berekfurdo, and in the Serbian sector at c. 10 km at Zrenjanin); the palaeochannel is up to 600 m wide and locally more than 14 m deep at Berekfurdo in Hungary [30] and up to 2 km wide in Serbia. There seems to be a lateral morphological transition into a braided system (2) at Berekfurdo, which could mean that systems 2 and the terminal part of 3a were contemporaneous. The floodplain deposits at a depth of 6 to 7 m at Zrenjanin have been dated by OSL at 33–32 ka. The uncalibrated radiocarbon age of c. 29 ka BP for the meander fill in the Berekfurdo channel [30] fits with the OSL dates obtained at Zrenjanin, but conflicts with younger ages (25–22 ka) of adjacent dissected floodplain deposits (belonging to system 1 [30] and unpublished IRSL dates for the uppermost point-bar deposits at Berekfurdo (14.3 ± 1.1 ka to 9.4 ± 2.1 ka [77]). However, the latter point-bar deposits reflect only very weak flow, as evidenced by the dominance of clayey flood deposits overlying very thin beds of fine sand without any pebbles (except locally derived clay pebbles), the absence of channelling structures, but the frequent occurrence of small ripples draped by clay; thus, they may have been rejuvenated by younger (Lateglacial) fluvial action towards the final stage of activity of that system (see below), which would explain why their young age obviously deviates from the older radiocarbon ages. In addition, the older ages of the Berekfurdo meander system (3a) are also inconsistent with the younger radiocarbon age (22–17 ka cal BP; see above) of the older or contemporaneous braided system (2) [30], although older OSL-ages (27 to 20 ka) from braided system 2 were also obtained [36] (see above). At any rate, the different dates from Berekfurdo remain inconsistent with each other. Rather than trying to reconcile the different age determinations, we favour a more generalized pattern of the fluvial evolution of system 3a. It assumes continuous activity from at least 33–32 ka until 22–17 ka when river activity slowed down (top of Berekfurdo meander) (Table 2). At that same terminal phase of system 3a, the meandering system would seem to have interfingered with braided system 2, which probably represents the outermost zone of the Sajo alluvial fan (Figure 2). Continuous meandering alluviation over that long period from c. 33 to c. 17 ka may explain the occurrence of many beds dated in that interval (e.g., [36]), occurring at different positions in the system. They may even include dated material from 25–22 ka attributed to system 1 [30]. Moreover, transitions between a braided and meandering pattern exist at present at the Ukrainian–Hungarian border and occurred also during the Lateglacial in the Maros river (tributary of the Tisa near to the Hungarian–Serbian border) [78]. The advantage of this hypothesis of fluvial evolution is that we can assemble in a single framework all absolute dates (radiocarbon and OSL) from the two regions within their error bars.

Table 2. Summary of the fluvial systems 1 to 3d, and their periods of activity in the Tis(z)a River.

Fluvial Phase	Fluvial Systems with Type-Sites	Periods of Activity
3d	Meanders W of Mužlja (lower Tisa)	Late Glacial
3c	Meanders of Tiszaörs (middle Tisza)—Mužlja (lower Tisa)	15.6 ka to start of Younger Dryas
3b	Meanders of Kunmadaras (middle Tisza)	19–17 ka
3a	Meanders of Zrenjanin (lower Tisa)—Berekfurdo (middle Tisza)	From c. 33 to 17 ka
2	'Sajo alluvial fan'—braided	c. (27–)22–17 ka
1	Large meanders of Meggyes	>28 ka

A subsequent younger phase (3b) within this system of meanders clearly dissects the meanders of phase 3a. It has distinctly smaller wavelengths than the previous generation 3a, in the range of 4–5 km at Kunmadaras. In the lower Tisa, the oldest phase eroding the Zrenjanin terrace is represented by a terrace remnant of very limited extent W of Zrenjanin. The radiocarbon age of the Kunmadaras

system is 19.26–16.25 ka BP, as derived from the meander fill, but 15.26–13.56 ka BP for adjacent sediments (c. 19–17 ka after calibration). It has been suggested that the ages of the meander fill are probably a few thousand years too old [30]. The Tiszacsege meander and a series of meanders nearby (of comparable size) may correspond with the Kunmadaras meander; the pollen diagram Tiszacsege (discussed by Kasse et al. [30]) shows the fill of a meander scar that started at the final part of the Pleniglacial). Fills of large meanders, radiocarbon-dated between 25 and 20 ka, were previously reported [34,36,79] in the neighbourhood of Polgar at c. 50 km north of our study area. They could be correlated with phase 3a or 3b.

The next, third phase (3c) has smaller meander wavelengths but still occurs at the same topographic level. It is IRSL-dated for the upper point-bar series at Mužlja, giving an age of 15.6–15.3 ka [49] (Figure 9), which is definitely younger than the Kunmadaras terrace. It may correspond with the Tiszaörs meander (wavelength 3–4 km) of the middle Tisza which is radiocarbon-dated between 17.9 and 13.8 ka BP using detritus from within point-bar deposits [30]. However, the pollen diagram of the meander fill at Tiszaörs shows that infill started only in the final part of the Lateglacial [30], which is certainly much younger than the Tiszacsege meander (system 3b). We assume that the meander may have been active from the end of the Pleniglacial until the Lateglacial after which the pollen registration started and thus—accepting the radiocarbon ages—we correlate the Tiszaörs meander with the Muzlja terrace. The period between 17 and 14 ka was a very dry interval that led to reduced vegetation and river activity [34,65,80].

In the lower Tisa, the next terrace system W of Mužlja (3d) occurs some 2 m lower (at c. 75 m elevation) than the previous one at Mužlja (3c). The meander size seems again to be somewhat reduced in comparison with the previous phase. It is not recognized in the study region of the middle Tisza. Taking into account the age of the Mužlja terrace, we infer a Lateglacial age for system 3d (Table 2).

A strikingly abrupt change towards the most recent phase, which dates from the Holocene, is found in the middle Tisza. In that area, this system of small meanders (4) is separated from the next older terrace by a sharp scarp of about 4 m. In both areas, there is a strong reduction in meander length, channel depth and width (which decreased to 500–400 m) and lateral and vertical erosion of the system. It persisted until pre-modern time, i.e., until human intervention.

Table 2 summarizes the different systems in the present valley belt with their derived ages. The most striking features are the clear phase of incision slightly prior to 33 ka, followed by a rather long period of alluviation in a system of very large meanders (system 3a). This system persisted until c. 17 ka, followed by relatively rapid (relative) decrease of meander size in several stages 3b–d ending in the Lateglacial. A sharp decrease of meander size occurred at the transition to the Holocene.

6. Discussion

6.1. General Characteristics of the Middle and Lower Tis(z)a River Systems

The general fluvial pattern is that of a dominantly meandering system in which accumulation and erosion seem to have alternated. The subsidence of the Pannonian Basin led to low river gradients and thus to generally low-energy conditions that favoured a meandering river pattern. The accumulative activity is interrupted once by the deep erosion of the meanders just before system 3a (Berekfurdo, Tiszaszege). Its age could not be established precisely but is estimated to be shortly before 33 ka. Similar to but possibly slightly earlier than in more northern regions [10], the onset of frozen-ground conditions and the delayed response of deteriorating vegetation cover in the Pannonian Basin may have induced considerable erosion before system 3 alluviation, leading to increased runoff with a still low sediment supply [8]. At the time of degradation of frozen soils (towards the end of the Weichselian and/or the transition to the Holocene) and subsequent increase of soil permeability, the runoff decreased, and meanders reduced their dimensions due to lower and more steady discharges [80].

The oldest recorded systems in the present-day valley belt (systems 1 and 3a) date from the end of the Weichselian Middle Pleniglacial and show meandering patterns that are relatively large compared to

later patterns [30,33]. Because of a relatively thick cover of fine-grained flood-sediment, it is not possible to determine precise form parameters such as wavelength or curvature radius. A rough estimate of that system is between 6 and 10 km in wavelength. Postdating the meanders at Berekfurdo and Zrenjanin (3a), the size of the meanders decreased successively in the meander systems from 3b to 3c in the middle Tisza (Kunmadaras and Tiszaörs meanders). In the lower Tisa, this evolution from 3b to 3d is less distinct, as the preserved terrace remnants are too small to be measured (meanders W of Mužlja). In contrast, the Holocene meanders in both regions are considerably smaller than all pre-Holocene systems. This fact is very common in many river systems ([10,81,82] and references therein).

Comparable large meanders have been described from the Russian Plain and mid-Russian Uplands [83–85], as exemplified by the Late Valdaian (~Weichselian) Seim river with meander wavelengths of 5 to 6 km, an amplitude of 4 km and channel widths 15 times the recent ones [83]. In that river, the elevation difference between the highest levels and deepest point of the palaeo-channel amounts to 14 m. In that same river valley in the southern Russian Plain, younger meanders with Lateglacial valley fills show a reduction of the wavelength to 1.3 km, while the Holocene meander dimensions decreased considerably [84]. That Holocene size reduction is absent in the northeastern Russian Plain, which is still in the modern permafrost zone [83].

Explaining the large meander sizes requires consideration of the specific energy conditions in the fluvial systems during the Middle Pleniglacial (~MIS 3) and early Late Pleniglacial (~MIS 2). The available energy for meander development is especially determined by the discharge and the river gradient [26,86] as applied for the Tisza by Petrovszki et al. [87]. Due to the geographical position of the Tis(z)a within the Pannonian Basin, river slopes are very low (see below). With respect to the runoff in this region, it may further be assumed that in a continental environment, the soils were frozen and thus impervious, at least for a considerable part of the year, but especially after the relatively cold winters [2,28]. These conditions may have been present in the Middle Pleniglacial and even more pronounced during the Late Pleniglacial when this region was situated at the margins of sporadic to discontinuous permafrost [40,41]. In addition, peak discharges may have increased due to the thaw of glacier ice in the Carpathians, feeding the Tisza catchment. Also, the rapid and spatially extensive thaw of snow cover in the low-relief setting of the Hungarian Plain may have contributed to high discharges in spring, as they have been, e.g., up to eight times larger at that time than at present in the Russian Plain [83,84]. In the Russian systems, frozen-soil conditions were probably even harsher than in western regions, while the topography was subdued in an environment of thermokarst depressions [85].

Furthermore, it is striking that in the Serbian Tisa and the Russian systems, no braided-river patterns are present during the Late Pleniglacial. Also, in the middle Tisza, a braided system was only occasionally present (see below). This contrasts with most river systems in other West European cold-temperate regions [10,22,88] (more examples in Kasse et al. [30], p. 192). Although the impact of frozen soil may have been similar in both regions during that period, the river gradients in West Europe were generally higher, even in lowlands (e.g., 0.2–0.3 m.km^{-1} and c. 0.15 m.km^{-1} for the lower Maas river and the middle Warta river in Poland, respectively [81], versus 0.02–0.15 m.km^{-1} for the Tisza river). In addition, braided development requires, in general, a relatively high sedimentation bedload which is favoured by the absence of vegetation. As the tundra vegetation in West Europe was more sparsely developed, in contrast with the well-developed steppe or even forest-steppic vegetation in central and eastern Europe, it is logical to assume less bedload sediment supply to the rivers in the latter regions. A relatively denser vegetation cover, together with the very low river gradients, may thus explain the absent tendency for braiding pattern development in those regions during the Late Pleniglacial.

6.2. Intercomparison between the Middle and Lower Tis(z)a

The general characteristics of stream patterns towards the end of the Lateglacial and the transition to the Holocene are similar in both the middle and lower Tis(z)a in Hungary and Serbia. Despite the

difficulties in absolute dating of individual systems and the discontinuous nature of fluvial deposition, the trends in the evolution of the Tis(z)a in Hungary and Serbia occur in a parallel manner.

There is one specific difference, however, which is the existence of a braided system (2) during the Late Pleniglacial in the middle Tisza in contrast to the lower Tisa. This braided system in the middle Tisza seems to be of local significance and restricted to a limited period of time. Apart from the theoretical possibility of the later removal of braided deposits and river patterns in the lower Tisa, the particular location of that braided system at the southern margin of the alluvial fan at the confluence of the Sajo and Tisza Rivers should be mentioned. In addition, different energy conditions exist in the two regions. Applying the same theories of drainage pattern development as described above to explain the dominant meandering systems during the last glacial period, topographical conditions may again provide a plausible explanation for the absence of a braided pattern in the lower Tisa. Especially striking is the strongly reduced longitudinal gradient in Serbia, which at present is 1.86 cm/km [31], when compared to the gradient in the middle Tisza of 15 cm/km in central to north Hungary [30], gradually diminishing to 5–10 cm/km in a zone of intense subsidence in south-eastern Hungary [35]. In contrast, it is not feasible to invoke a substantially different vegetation cover between the latter two regions. Thus, the strongly reduced stream power in a downstream direction is supposed to be the main reason for the persistent formation of a meandering pattern, uninterrupted by braiding, in the lower Tisa during the Late Pleniglacial.

As a general conclusion, and as a result of the further studies of the Tis(z)a system in Hungary and Serbia, the importance of timescale (cf. [5]) is confirmed here. In the long term, the tectonic framework (basin development) and resulting topography have determined the available energy in this fluvial system. At a shorter timescale, climatic conditions (including their effects on vegetation and soil frost) have left a distinct imprint. Finally, looking at more detailed spatial and temporal scales, local variations of topography and sediment availability may be responsible for further shaping the river morphology [22,81] next to intrinsic variables as thresholds and delay times.

7. Conclusions

Several characteristics of fluvial development found in the continental low-relief setting of the Tis(z)a river are identical to the cold-temperate conditions in the West-European lowlands. In this respect, the sharp decrease in meander size at the Weichselian to Holocene transition is striking. However, there are also a few differences, such as the near absence of braided river patterns and the existence of exceptionally large meanders during the Weichselian Middle and Late Pleniglacial.

Previous studies have frequently stressed the importance of climate and tectonic movement as external factors in fluvial morphological development. This study of the Tis(z)a valley illustrates that, for a reliable understanding of fluvial evolution, the impact of climate on fluvial processes and morphology cannot be limited to general estimates or averages but also needs to be effectively specified in detail, for instance including the continental conditions with cold winters and relatively warm summers in the Tis(z)a catchment and in the Russian plain. In addition, they have to be supplemented with indirect climate variables (as vegetation, frozen soil and snow cover), while the impact of tectonic subsidence, and its variability within one catchment as in the Tis(z)a, has to be specified in semi-direct variables such as the longitudinal river gradient and relief intensity. This study confirms the impact of varying conditions of climate and topography at a local and regional level on fluvial development.

Author Contributions: J.V.: conceptualization, field data collection, interpretation, writing original draft; K.K. and G.G.: conceptualization, field data collection, interpretation; S.B.: field data collection, paleobotanical interpretation; S.M.: field data collection, interpretation; D.V. and D.P.: OSL-dating.

References

1. Büdel, J. *Klima-Geomorphologie*; Gebrüder Bornträger: Berlin, Germany, 1977; p. 304.
2. Vandenberghe, J. The relation between climate and river processes, landforms and deposits during the Quaternary. *Quat. Int.* **2002**, *91*, 17–23. [CrossRef]
3. Starkel, L. Climatically controlled terraces in uplifting mountain areas. *Quat. Sci. Rev.* **2003**, *22*, 2189–2198. [CrossRef]
4. Vandenberghe, J. Changing fluvial processes under changing periglacial conditions. *Z. Geomorphol.* **1993**, *88*, 17–28.
5. Vandenberghe, J. Timescales, climate and river development. *Quat. Sci. Rev.* **1995**, *14*, 631–638. [CrossRef]
6. Bridgland, D.R.; Allen, P. A revised model for terrace formation and its significance for the early middle Pleistocene terrace aggradations of north-east Essex, England. In *The Early Middle Pleistocene in Europe*; Turner, C., Ed.; Balkema: Rotterdam, The Netherlands, 1996; pp. 121–134.
7. Maddy, D.; Bridgland, D.; Westaway, R. Uplift-driven valley incision and climate-controlled river terrace development in the Thames Valley, UK. *Quat. Int.* **2001**, *79*, 23–36. [CrossRef]
8. Vandenberghe, J. The fluvial cycle at cold-warm-cold transitions in lowland regions: A refinement of theory. *Geomorphology* **2008**, *98*, 275–284. [CrossRef]
9. Vandenberghe, J. River terraces as a response to climatic forcing: Formation processes, sedimentary characteristics and sites for human occupation. *Quat. Int.* **2015**, *370*, 3–11. [CrossRef]
10. Mol, J.; Vandenberghe, J.; Kasse, C. River response to variations of periglacial climate. *Geomorphology* **2000**, *33*, 131–148. [CrossRef]
11. Pan, B.; Su, H.; Hu, Z.; Hu, X.; Gao, H.; Li, J.; Kirby, E. Evaluating the role of climate and tectonics during non-steady incision of the Yellow River: Evidence from a 1.24 Ma terrace record near Lanzhou, China. *Quat. Sci. Rev.* **2009**, *28*, 3281–3290. [CrossRef]
12. Wang, X.; Van Balen, R.; Yi, S.; Vandenberghe, J.; Lu, H. Differential tectonic movements in the confluence area of the Huang Shui and Huang He rivers (Yellow River), NE Tibetan Plateau, as inferred from fluvial terrace positions. *Boreas* **2014**, *43*, 469–484. [CrossRef]
13. Kemp, J.; Pietsch, T.; Gontz, A.; Oley, J. Lacustrine-fluvial interactions in Australia's Riverine Plains. *Quat. Sci. Rev.* **2017**, *166*, 352–362. [CrossRef]
14. Marsh, P.; Woo, M.K. Snowmelt, glacier melt and High Arctic streamflow regimes. *Can. J. Earth Sci.* **1981**, *18*, 380–1384. [CrossRef]
15. Cordier, S.; Frechen, M.; Harmand, D. Dating fluvial erosion: Fluvial response to climate change in the Moselle catchment (France, Germany) since the Late Saalian. *Boreas* **2014**, *43*, 450–468. [CrossRef]
16. Cordier, S.; Adamson, K.; Delmas, M.; Calvet, M.; Harmand, D. Of ice and water: Quaternary fluvial response to glacial forcing. *Quat. Sci. Rev.* **2017**, *166*, 57–73. [CrossRef]
17. Ballantyne, C.K. A general model of paraglacial landscape response. *Holocene* **2002**, *12*, 371–376. [CrossRef]
18. Owczarek, P.; Nawrot, A.; Migala, K.; Malik, I.; Korabiewski, B. Floodplain responses to contemporary climate change in small High-Arctic basins (Svalbard, Norway). *Boreas* **2014**, *43*, 384–402. [CrossRef]
19. Dogan, U. Fluvial response to climate change during and after the Last Glacial Maximum in Central Anatolia, Turkey. *Quat. Int.* **2010**, *222*, 221–229. [CrossRef]
20. Avcin, N.; Vandenberghe, J.; van Balen, R.T.; Kıyak, N.; Öztürk, T. Tectonic and Climatic Controls on Quaternary Fluvial Processes and Terrace Formation in a Mediterranean Setting: The Göksu River, Southern Anatolia. *Quat. Res.* **2018**. under review.

21. Hughes, K.; Croke, J. How did rivers in the wet tropics (NE Queensland, Australia) respond to climate changes over the past 30000 years? *J. Quat. Sci.* **2017**, *32*, 744–759. [CrossRef]

22. Kasse, C. Depositional model for cold-climate tundra rivers. In *Palaeohydrology and Environmental Change*; Benito, G., Baker, V.R., Gregory, K.J., Eds.; Wiley and Sons: Chichester, UK, 1998; pp. 83–97.

23. Rose, J.; Meng, X. River activity in small catchments over the last 140 ka, North-east Mallorca, Spain. In *Fluvial Processes and Environmental Change*; Brown, A.G., Quine, T.A., Eds.; Wiley & Sons: Chichester, UK, 1999; pp. 91–102.

24. Olszak, J. Evolution of fluvial terraces in response to climate change and tectonic uplift during the Pleistoce: Evidence from Kamienica and Ochotnica River valleys (Polish Outer Carpathians). *Geomorphology* **2011**, *129*, 71–78. [CrossRef]

25. Stange, K.M.; van Balen, R.T.; Carcaillet, J.; Vandenberghe, J. Terrace staircase development in the Southern Pyrenees Foreland: Inferences from 10Be terrace exposure ages at the Segre River. *Glob. Planet. Change* **2013**, *101*, 97–112. [CrossRef]

26. Schumm, S. *The Fluvial System*; Wiley-Interscience: New York, NY, USA, 1977; p. 338.

27. Van Huissteden, J. *Tundra Rivers of the Last Glacial: Sedimentation and Geomorphological Processes during the Middle Pleniglacial in the Dinkel Valley (Eastern Netherlands)*; Rijks Geologische Dienst: Haarlem, The Netherlands, 1990; Volume 44, pp. 3–138.

28. Vandenberghe, J. A typology of Pleistocene cold-based rivers. *Quat. Int.* **2001**, *179*, 111–121. [CrossRef]

29. Bridgland, D.R.; Westaway, R. Preservation patterns of Late Cenozoic fluvial deposits and their implications: Results from IGCP 449. *Quat. Int.* **2008**, *189*, 5–38. [CrossRef]

30. Kasse, C.; Bohncke, S.J.P.; Vandenberghe, J.; Gabris, G. Fluvial style changes during the last glacial—Interglacial transition in the middle Tisza valley (Hungary). *Proc. Geol. Assoc.* **2010**, *121*, 180–194. [CrossRef]

31. Popov, D.; Markovic, S.; Strbac, D. Generations of meanders in Serbian part of Tisa valley. *J. Geogr. Inst. Jovan Cvijic SASA* **2008**, *58*, 29–41. [CrossRef]

32. Nádor, A.; Lantos, M.; Tóth-Makk, Á.; Thamó-Bozsó, E. Milankovitch-scale multi-proxy records from fluvial sediments of the last 2.6 Ma, Pannonian Basin, Hungary. *Quat. Sci. Rev.* **2003**, *22*, 2157–2175. [CrossRef]

33. Gabris, G.; Nador, A. Long-term fluvial archives in Hungary: Response of the Danube and Tisza rivers to tectonic movements and climatic changes during the Quaternary: A review and new synthesis. *Quat. Sci. Rev.* **2007**, *26*, 2758–2782. [CrossRef]

34. Timar, G.; Sümegi, P.; Horvath, F. Late Quaternary dynamics of the Tisza river: Evidence of climatic and tectonic controls. *Tectonophysics* **2005**, *410*, 97–110. [CrossRef]

35. Nádor, A.; Thamó-Bozsó, E.; Magyari, A.; Babinszki, E. Fluvial responses to tectonics and climate change during the Late Weichselian in the eastern part of the Pannonian Basin (Hungary). *Sediment. Geol.* **2007**, *201*, 174–192. [CrossRef]

36. Gabris, G.; Horvath, E.; Novothny, A.; Ruszkiczay-Rüdiger, Z. Fluvial and Aeolian landscape evolution in Hungary-results of the last 20 years research. *Neth. J. Geosci.* **2012**, *91*, 111–128. [CrossRef]

37. Willis, K.J.; Rudner, E.; Sümegi, P. The Full-Glacial Forests of Central and Southeastern Europe. *Quat. Res.* **2000**, *53*, 203–213. [CrossRef]

38. Sümegi, P.; Krolopp, E. Quatermalacological analyses for modelling of the Upper Weichselian paleoenvironmental changes in the Carpathian Basin. *Quat. Int.* **2002**, *91*, 53–63. [CrossRef]

39. Bacso, N. *Climate of Hungary*; Akademiai Kiado: Budapest, Hungary, 1959; p. 302. (In Hungarian)

40. Fábián, S.A.; Kovács, J.; Varga, G.; Sipos, G.; Horváth, Z.; Thamó-Bozsó, E.; Tóth, G. Distribution of relict permafrost features in the Pannonian Basin, Hungary. *Boreas* **2014**, *43*, 722–732. [CrossRef]

41. Vandenberghe, J.; French, H.M.; Gorbunov, A.; Marchenko, S.; Velichko, A.A.; Jin, H.; Cui, Z.; Zhang, T.; Wan, X. The Last Permafrost Maximum (LPM) map of the Northern Hemisphere: Permafrost extent and mean annual air temperatures, 25–17 ka BP. *Boreas* **2014**, *43*, 652–666. [CrossRef]

42. Royden, L.H.; Horvath, F. The Pannonian Basin. A case study in basin evolution. *AAPG Memoirs* **1988**, *45*, 394.

43. Horvath, F.; Cloetingh, S. Stress induced late-stage subsidence anomalies in the Pannonian Basin. *Tectonophysics* **1996**, *266*, 287–300. [CrossRef]

44. Bada, G.; Horvath, F. On the structure and tectonic evolution of the Pannonian Basin and surrounding orogens. *Acta Geol. Hung.* **2001**, *44*, 301–327.

45. Pecsi, M. *Entwicklung und Morphologie des Donautales in Ungarn*; Akademiai Kiado: Budapest, Hungary, 1959; p. 359. (In Hungarian)

46. Thamo-Bozso, E.; Murray, A.A.; Nador, A.; Magyari, A.; Babinszki, E. Investigation of river network evolution using luminescence dating and heavy-mineral analysis of Late Quaternary fluvial sands from the Great Hungarian Plain. *Quat. Geochronol.* **2007**, *2*, 168–173. [CrossRef]

47. Gabris, G. Pleistocene evolution of the Danube in the Carpathian Basin. *Terra Nova* **1994**, *6*, 495–501. [CrossRef]

48. Konert, M.; Vandenberghe, J. Comparison of laser grain size analysis with pipette and sieve analysis: A solution for the underestimation of the clay fraction. *Sedimentology* **1997**, *44*, 523–535. [CrossRef]

49. Popov, D.; Vandenberghe, D.A.G.; Marković, S.B. Luminescence dating of fluvial deposits in Vojvodina, N Serbia: First results. *Quat. Geochronol.* **2012**, *13*, 42–51. [CrossRef]

50. Bøtter-Jensen, L.; Andersen, C.E.; Duller, G.A.T.; Murray, A.S. Developments in radiation, stimulation and observation facilities in luminescence measurements. *Radiat. Meas.* **2003**, *37*, 535–541. [CrossRef]

51. Lapp, T.; Kook, M.; Murray, A.S.; Thomsen, K.J.; Buylaert, J.-P.; Jain, M. A new luminescence detection and stimulation head for the Risø TL/OSL reader. *Radiat. Meas.* **2015**, *81*, 178–184. [CrossRef]

52. Duller, G.A.T. Distinguishing quartz and feldspar in single grain luminescence measurements. *Radiat. Meas.* **2003**, *37*, 161–165. [CrossRef]

53. Murray, A.S.; Wintle, A.G. Luminescence dating of quartz using an improved single-aliquot regenerative-dose protocol. *Radiat. Meas.* **2000**, *32*, 57–73. [CrossRef]

54. Murray, A.S.; Wintle, A.G. The single aliquot regenerative dose protocol: Potential for improvements in reliability. *Radiat. Meas.* **2003**, *37*, 377–381. [CrossRef]

55. Hossain, S.M. A Critical Comparison and Evaluation of Methods for the Annual Radiation Dose Determination in the Luminescence Dating of Sediments. Ph.D. Thesis, Ghent University, Gent, Belgium, 2003.

56. Vandenberghe, D. Investigation of the Optically Stimulated Luminescence Dating Method for Application to Young Geological Samples. Ph.D. Thesis, Ghent University, Gent, Belgium, 2004.

57. De Corte, F.; Vandenberghe, D.; De Wispelaere, A.; Buylaert, J.-P.; Van den haute, P. Radon loss from encapsulated sediments in Ge gamma-ray spectrometry for the annual radiation dose determination in luminescence dating. *Czechoslov. J. Phys.* **2006**, *56*, D183–D194. [CrossRef]

58. Adamiec, G.; Aitken, M. Dose-rate conversion factors: Update. *Ancient TL* **1998**, *16*, 37–50.

59. Mejdahl, V. Thermoluminescence dating: Beta-dose attenuation in quartz grains. *Archaeometry* **1979**, *21*, 61–72. [CrossRef]

60. Aitken, M.J. *Thermoluminescence Dating*; Academic Press Inc.: London, UK, 1985; p. 359.

61. Vandenberghe, D.; De Corte, F.; Buylaert, J.-P.; Kucera, J.; Van den haute, P. On the internal radioactivity in quartz. *Radiat. Meas.* **2008**, *43*, 771–775. [CrossRef]

62. Prescott, J.R.; Hutton, J.T. Cosmic ray contributions to dose rates for luminescence and ESR dating: Large depths and long-term time variations. *Radiat. Meas.* **1994**, *23*, 497–500. [CrossRef]

63. Aitken, M.J. Thermoluminescence age evaluation and assessment of error limits: Revised system. *Archaeometry* **1976**, *18*, 233–238. [CrossRef]

64. Aitken, M.J.; Alldred, J.C. The assessment of error limits in thermoluminescence dating. *Archaeometry* **1972**, *14*, 257–267. [CrossRef]

65. Vandenberghe, D.; Kasse, C.; Hossain, S.M.; De Corte, F.; Van den haute, P.; Fuchs, M.; Murray, A.S. Exploring the method of optical dating and comparison of optical and 14C ages of Late Weichselian coversands in the southern Netherlands. *J. Quat. Sci.* **2004**, *19*, 73–86. [CrossRef]

66. Vandenberghe, J.; Bohncke, S.; Lammers, W.; Zilverberg, L. Geomorphology and palaeoecology of the Mark valley (southern Netherlands). I Geomorphological valley development during the Weichselian and Holocene. *Boreas* **1987**, *16*, 55–67. [CrossRef]

67. Novotny, A.; Frechen, M.; Horvath, E.; Wacha, L.; Rolf, C. Investigating the penultimate and last glacial cycles of the Süttö loess section (Hungary) using luminescence dating, high-resolution grain size, and magnetic susceptibility data. *Quat. Int.* **2011**, *234*, 75–85. [CrossRef]

68. Bokhorst, M.; Vandenberghe, J.; Sümegi, P.; Lanczont, M.; Gerasimenko, N.P.; Matviishina, Z.N.; Markovic, S.B.; Frechen, M. Atmospheric circulation patterns in Central and Eastern Europe during the Weichselian Pleniglacial inferred from loess grain-size records. *Quat. Int.* **2011**, *234*, 62–74. [CrossRef]

69.	Vandenberghe, J.; Sun, Y.; Wang, X.; Abels, H.A.; Liu, X. Grain-size characterization of reworked fine-grained aeolian deposits. *Earth Sci. Rev.* **2018**, *177*, 43–52. [CrossRef]

70.	Wang, X.; Ma, J.; Yi, S.; Vandenberghe, J.; Dai, Y.; Lu, H. Interaction of fluvial and aeolian sedimentation processes and response to climate change since the last glacial in a semi-arid environment along the Yellow River. *Quat. Res.* **2018**, *1*. [CrossRef]

71.	Verdonk, S. Fluvial development of lithology and geomorphology of Tisza river terraces since the last glacial maximum in Vojvodina, Serbia. BSc Thesis, Faculty of Earth and Life Sciences, Vrije Universiteit, Amsterdam, The Netherlands, 2003.

72.	Marković, S.B.; Bokhorst, M.; Vandenberghe, J.; McCoy, W.D.; Oches, E.A.; Hambach, U.; Gaudenyi, T.; Jovanović, M.; Stevens, T.; Zöller, L.; et al. Late Pleistocene loess-palaeosol sequences in the Vojvodina region, north Serbia. *J. Quat. Sci.* **2008**, *23*, 73–84. [CrossRef]

73.	Marković, S.B.; Stevens, T.; Kukla, G.J.; Hambach, U.; Fitzsimmons, K.E.; Gibbard, P.; Buggle, B.; Zech, M.; Guo, Z.T.; Hao, Q.Z.; et al. The Danube loess stratigraphy—New steps towards the development of a pan-European loess stratigraphic model. *Earth Sci. Rev.* **2015**, *148*, 228–258. [CrossRef]

74.	Popov, D.; Marković, S.B.; Jovanović, M.; Mesaroš Arsenović, D.; Stankov, U.; Gubik, D. Geomorphological investigations and GIS approach of the Tamiš loess plateau, Banat region (northern Serbia). *Geogr. Pannonica* **2012**, *16*, 1–9. [CrossRef]

75.	Jain, M.; Murray, A.S.; Bøtter-Jensen, L. Optically stimulated luminescence dating: How significant is incomplete light exposure in fluvial environments? *Quaternaire* **2004**, *15*, 143–157. [CrossRef]

76.	Borsy, Z. Evolution of the alluvial fans of the Alföld. In *Alluvial Fans: A Field Approach*; Rachocki, A.H., Church, M., Eds.; Wiley and Sons Ltd.: Chichester, UK, 1990; pp. 229–246.

77.	Frechen, M.; Leibniz Institute for Applied Geophysics, Hannover, Germany. Personal communication, 2003.

78.	Berec, B.; Gábris, G. A Maros hordalékkúp bánsági szakasza (Alluvial fan of Maros River in Banat, Serbia–Romania). In *Kárpát-Medence: Természet, Társadalom, Gazdaság (Carpathian Basin: Nature, Society, Economy)*; Frisnyák, S., Gál, A., Eds.; Nyíregyháza–Szerencs: Nyíregyháza, Hungary, 2013; pp. 51–64. (In Hungarian)

79.	Davis, B.A.S.; Passmore, D.G. Upper Tisza Project: Radiocarbon analyses of Holocene alluvial and lacustrine sediments. In *Interim Report on Current Analyses to the Excavation and Fieldwork Committee*; University of Newcastle: Callaghan, Australia, 1998; Volume 7.

80.	Kasse, C. Cold-climate aeolian sand-sheet formation in north-western Europe (c. 14-12.4 ka): A response to permafrost degradation and increased aridity. *Permafr. Periglac. Process.* **1997**, *8*, 295–311. [CrossRef]

81.	Vandenberghe, J.; Kasse, C.; Bohncke, S.; Kozarski, S. Climate-related river activity at the Weichselian-Holocene transition: A comparative study of the Warta and Maas rivers. *Terra Nova* **1994**, *6*, 476–485. [CrossRef]

82.	Kasse, C.; Vandenberghe, J.; Bohncke, S. Climatic change and fluvial dynamics of the Maas during the Late Weichselian and Early Holocene. In *European River Activity and Climatic Change during the Lateglacial and Early Holocene*; Frenzel, B., Vandenberghe, J., Kasse, C., Bohncke, S., Gläser, B., Eds.; Gustav Fischer: Jena, Germany, 1995; Volume 14, pp. 123–150.

83.	Sidorchuk, A.; Borisova, O.; Panin, A. Fluvial response to the Late Valdai/Holocene environmental change on the East European Plain. *Glob. Planet. Change* **2001**, *28*, 303–318. [CrossRef]

84.	Sidorchuk, A.; Panin, A.; Borisova, O. Morphology of river channels and surface runoff in the Volga River basin (East European Plain) during the Late Glacial period. *Geomorphology* **2009**, *113*, 137–157. [CrossRef]

85.	Borisova, O.; Sidorchuk, A.; Panin, A. Palaeohydrology of the Seim River basin, Mid-Russian Upland, based on palaeochannel morphology and palynological data. *Catena* **2006**, *66*, 53–73. [CrossRef]

86.	Leopold, L.B.; Wolman, L.G.; Miller, J. *Fluvial Processes in Geomorphology*; W.H. Freeman and Co.: San Francisco, CA, USA, 1964; p. 522.

87. Petrovszki, J.; Timar, G.; Molnar, G. Is sinuosity a function of slope and bankfull discharge?—A case study of the meandering rivers in the Pannonian Basin. *Hydrol. Earth Syst. Sci. Discuss.* **2014**, *11*, 12271–12290. [CrossRef]

88. Van Huissteden, J.; Vandenberghe, J. Changing fluvial style of periglacial lowland rivers during the Weichselian Pleniglacial in the eastern Netherlands. *Z. Geomorphol.* **1988**, *71*, 131–146.